

TKN

Telecommunication
Networks Group



Technical University Berlin

Telecommunication Networks Group

Adaptive Coding as a Means to
increase Multi-User OFDM
Control Channel Reliability

Mathias Bohge, Anders Furuskär,
Magnus Lundevall

bohge@tkn.tu-berlin.de, anders.furuskar@ericsson.com,

magnus.lundevall@ericsson.com

Berlin, November 2007

TKN Technical Report TKN-07-005

TKN Technical Reports Series

Editor: Prof. Dr.-Ing. Adam Wolisz

Abstract

Dynamic mechanisms such as adaptive modulation and coding or scheduling have been shown to significantly improve the performance of cellular systems. This gain comes at the cost of additional signaling overhead that needs to be delivered from the transmitter to the receiver. In this paper, we explore a resource-constraint control channel that delivers resource assignments in a multi-cell environment with a frequency reuse of 1. It has been shown that despite the presence of co-channel interference signaling data can reliably be delivered to all users, if sufficient redundancy is added in order to protect the signalling data. In this paper, we present adaptive coding as a means to increase the control channel's reliability, while at the same time decreasing the necessary amount of redundancy. We introduce a new adaptive coding algorithm and show its benefits by comparing the related simulation results to the non-adaptive coding case.¹

¹This work has been supported by the German Ministry of Education and Science (BMBF) and Ericsson Research, Germany, in the context of the project ScaleNet.

Contents

1	Introduction	2
2	System Model	4
2.1	Physical Layer	4
2.2	User Data Multiplexing	4
2.3	Signaling Data Multiplexing	6
2.4	Wireless Channel Model	6
2.5	Link-to-System Model	7
3	Control Channel Configuration	8
3.1	Static Coding Configuration	8
3.2	Dynamic Coding Configuration	9
4	Simulation	11
4.1	Methodology	11
4.2	Results	11
5	Conclusions	17
	References	18

Chapter 1

Introduction

The performance increasing impact of dynamic resource allocation mechanisms in multi-user orthogonal frequency division multiplexing (MU-OFDM) systems has first been recognized in [1]. Since then it has thoroughly been studied in numerous papers for single, as well as multi-cell scenarios. It is well known that the gains come at the cost of additional signaling data, namely the resource allocation information that needs to be delivered to the receiver. As a consequence, system resources in terms of bandwidth or time need to be provided to form some kind of control channel. Four different factors decide on the amount of system resources that are necessary thereto: (1) the system setup, i.e. the number of available sub-carriers, modulation types, coding rates, etc.; (2) the wireless channel's dynamic, as the necessary signaling frequency is proportional to the channel state changes; (3) the granularity of the dynamic assignments; as well as (4) the redundancy that protects the resource allocation information. While in given network scenarios the first two factors are usually fixed, the latter two can be modified. Choosing a finer assignment granularity yields a better exploration of the system's frequency diversity, and thus a better system performance in terms of throughput. Selecting lower code-rates on the control channel accounts for more reliable control data delivery. This also has an impact on the user throughput, as user data is lost if the receiver holds erroneous allocation information. On the other hand both modifications increase the control channel's resource requirements and thus lower the system resources available for user data delivery. Hence, in order to optimize the system's performance in terms of user throughput, an optimal splitting of the overall amount of system resources into control channel and user data channel resources need to be determined.

However, most papers related to the system optimization topic assume the receiver to possess instant and perfect resource allocation information, which translates into an error-free zero resource consuming control channel model (e.g. [1–4]). So far, little research has been done on the application of an actual control channel. In [5, 6], it is shown that the gain achieved by adaptive sub-carrier allocation and power assignments is significantly larger than the increased overhead costs. But the studies are based on a single isolated cell environment and the channel is assumed to be fully reliable. Moreover, it is assumed, that the signaling data can be delivered in arbitrary units, without being bound to a certain control channel format.

In [7], we have explored a control channel model that includes significantly unreliable behavior - as its resources are reused in every single cell of the multi-cell setup. To the best of our knowledge, it is the first and only paper that considers an according system setup. The major contribution and paper conclusion is that despite the presence of co-channel interference, signaling data can reliably be de-

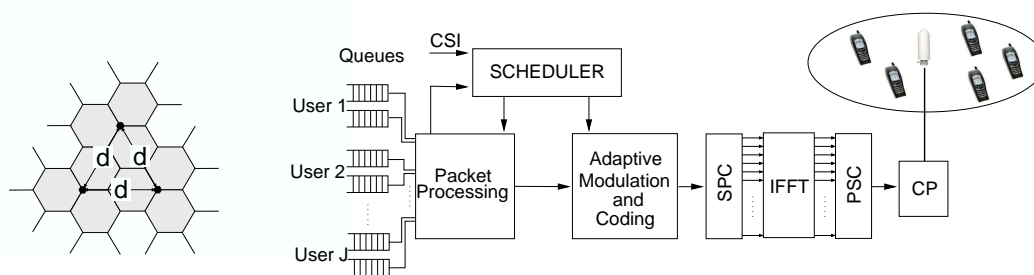


Figure 1.1: Co-channel interference scenario consisting of three base stations with three cells each (left). Adopted base station design (right).

livered to all users, if sufficient redundancy is added. Moreover, it has been shown that the amount of necessary redundancy can significantly be reduced if the control channel power per user is adaptively distributed.

In contrast and as an extension to that, we present adaptive coding as an alternative approach to improve the control channel performance in this paper. Control channel redundancy, i.e. the coding rate applied to the control data, is determined per user, based on the user's momentary channel state values. Our goal is to assure reliable control channel data delivery (in terms of meeting an expected target block error rate) for each user, while minimizing the control channel resource requirement (in terms OFDM symbols used for the control channel per frame-time). Exploring different levels of assignment granularity lies beyond the scope to this paper. Instead, we assume a system setup and assignment parameterization that equals those of the upcoming long term evolution (LTE) system. Accordingly, the considered control channel model configuration is equal to the one of LTE's physical downlink control channel (PDCCH) [8]. We perform our simulations on an LTE multi-user multi-cell system-level simulator developed at Ericsson, where the link states are translated into error probabilities according to a link-to-system model that has been presented in [9]. We compare the adaptive coding results with the results of an according system that relies on static coding. Moreover, we compare our adaptive coding approach to a recently introduced adaptive power approach.

The remainder of this paper is organized as follows: in the next section we introduce the system-, channel- and link-to-system models we adopt in our simulations. In Section 3 we present the control channel configuration and introduce our dynamic coding algorithm. Then, in Section 4 we describe our simulation scenario and present our simulation results. Finally, in Section 5 we conclude the paper.

Chapter 2

System Model

We consider a cellular system consisting of base stations and user terminals. The base stations are equidistantly located with the site-to-site distance d and operate in a synchronized mode. Each base station serves three cells leading to an overall number of C cells in the system. J terminals are distributed among all cells following a uniform distribution. The terminals feature two receive antennas and apply receive diversity. Each terminal is moving at a speed of v [m/s], but is supposed to be connected to exactly one cell per frame-time. We define c_j to be a function that delivers the cell entity c of the cell terminal j is currently connected to:

$$c_j : \mathcal{J} \rightarrow \mathcal{C}, j \rightarrow c, j \text{ connected to } c \quad (2.1)$$

2.1 Physical Layer

The system under consideration uses OFDM as transmission scheme for down-link data transmission. It has a total down-link bandwidth of B_{DL} [Hz] at center frequency f_c . The given bandwidth is split into S sub-carriers (with a spacing of B/S and a symbol length of T_s each). Prior to the transmission of the time domain OFDM symbol, a cyclic prefix of length T_g is added as guard interval. The maximum transmission power p_{max} per cell is distributed over the sub-carriers either statically (equal split) or dynamically.

2.2 User Data Multiplexing

Time is slotted into transmission time intervals (TTI) of duration T_{TTI} . During a single TTI, down-link data multiplexing is done by frequency division multiplexing (FDM), where the smallest addressable bandwidth-unit is a *resource block*. In the frequency domain, a resource block consists of a well defined number of adjacent sub-carriers. In the time domain, a resource block spans all OFDM symbols available for user data transmission of the respective TTI (see Figure 2.1). For each TTI, the base station scheduler decides on the resource block assignments per terminal according to a predefined scheduling policy. It also determines the power level, modulation type and coding rate per user, based on available channel state information (CSI). All scheduled terminals in cell c build the set \mathcal{J}_c . The size of \mathcal{J}_c at time t is given by $J_c^{(t)}$.

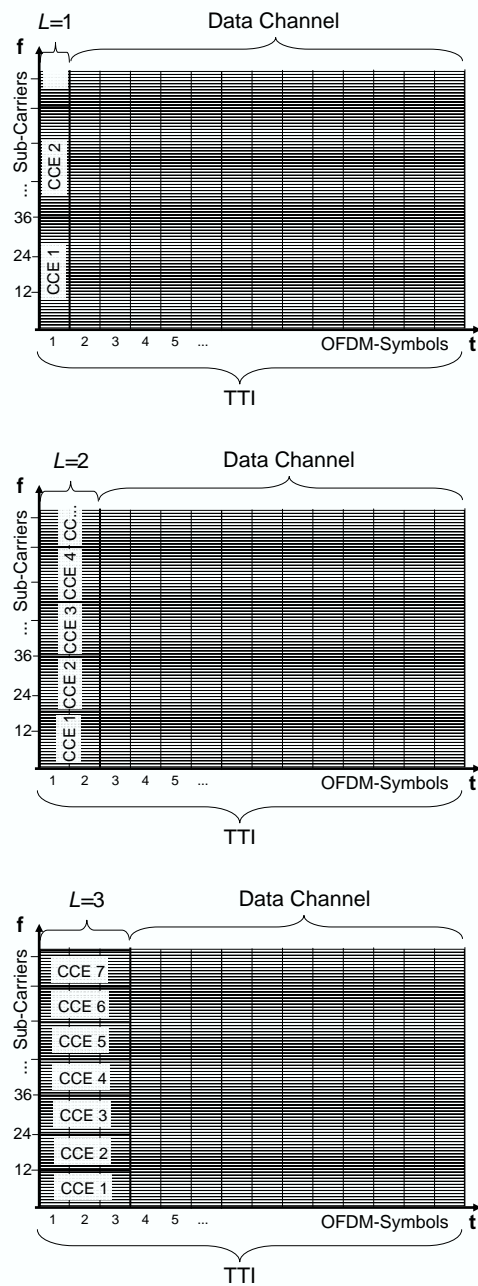


Figure 2.1: Each control channel element (CCE) consists of $\varphi=36$ resource elements (REs), where one resource element spans one sub-carrier in frequency and one OFDM symbol in time. Depending on the control channel sizes $L \in \{1, 2, 3\}$, one CCE spans 12, 24, or 36 sub-carriers, determined by the function l_L .

2.3 Signaling Data Multiplexing

In order to allow dynamic resource scheduling on the MAC layer, control signaling information needs to be delivered from the transmitting to the receiving side. Using this information, the receiving PHY must be configured such that data reception on the allocated resources is possible. We refer to the collection of necessary control information at the receiver side as a *down-link assignment*. For each user that the base station scheduler has scheduled for data delivery in the upcoming TTI, one such assignment must be delivered in advance. It contains the terminal's id for identification purposes, a cyclic redundancy check (CRC) value for error detection, a resource indicator identifying the terminal's resource block assignments, the transport block size, the id of the modulation type that is applied on the assigned resource blocks, as well as hybrid automatic repeat request (HARQ) information that is necessary to organize retransmissions. Note that the code-rate in use does not need to be signaled, as it can be derived from the other values. Depending on the resource assignments and the MAC layer's degree of flexibility, these down-link assignments might vary in size. In this paper, however, we define all assignments to be of the same size Ψ_{DL} .

We assume the down-link assignments to be delivered on a separate physical control channel. As described in [8], we assume this physical control channel to be time multiplexed with the physical down-link data channel, occupying the first L OFDM symbols of each TTI (see Figure 2.1). Hence, in each TTI an overall number of $L \times S$ resource elements (REs) is available for control signaling, where one RE spans one OFDM-symbol in the time domain and one sub-carrier in frequency. In order to lower the number of allocatable units, the REs are grouped into control channel elements (CCEs) of size φ REs. Note that one CCE spans all L OFDM symbols occupied by the control channel. Thus, the necessary number of sub-carriers to form a single CCE is a function of L :

$$l_L = \varphi/L \quad (2.2)$$

Also note that – in contrast to the way it is shown in Figure 2.1 – the l_L sub-carriers of a single CCE are non-adjacent, but spread across the frequency band in order to balance CCE channel quality (as described in [10]). Still, for the ease of presentation, we will stick to the depicted way of CCE aggregation and from now on refer to it as the *logical CCE domain*, whereas for channel state and interference calculations we need to remember that the CCE sub-carriers are spread in the *physical domain* using a logical-to-physical spreading function that differs among neighboring cells.

In order to allow different code-rates on the control channel, a varying amounts of CCEs can be aggregated per user (denoted as ϕ_j), where the per user code-rate ρ_j can be computed as follows:

$$\rho_j = \Psi_{DL}/2 \cdot \phi_j \cdot \varphi . \quad (2.3)$$

Note that there is a factor 2 in the denominator, since quadrature phase shift keying (QPSK) is consistently used as control channel modulation type.

2.4 Wireless Channel Model

Each terminal's instant signal-to-interference-plus-noise ratio (SINR) value per sub-carrier $\gamma_{j,s}^{(t)}$ varies over time due to its varying channel gain (reflecting path-loss, shadowing, and fading) and co-channel interference (CCI) caused by surrounding cells:

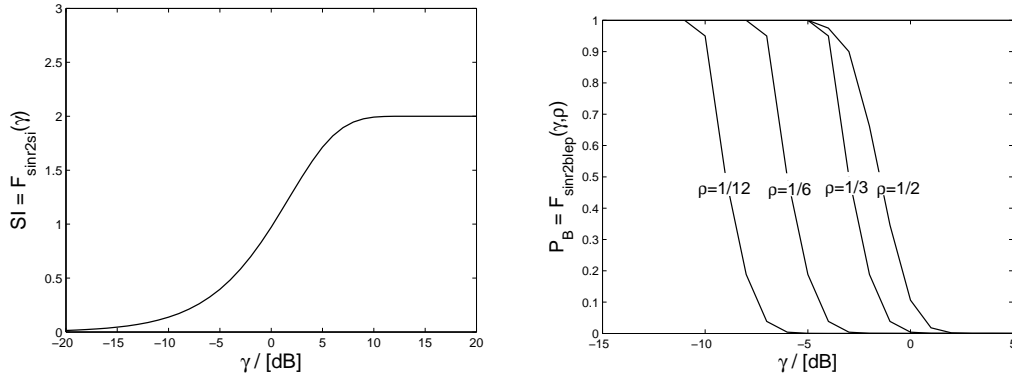


Figure 2.2: Link-to-system model functions $F_{\text{sinr2si}}(\gamma)$ (left) and $F_{\text{sinr2blep}}(\gamma, \rho)$ (right) for code rates $\rho = \{\frac{1}{12}, \frac{1}{6}, \frac{1}{3}, \frac{1}{2}\}$.

$$\gamma_{j,s}^{(t)} = \frac{p_j^{(t)} \cdot (h_{c_j,j,s}^{(t)})^2}{\sum_{c \neq c_j \in \mathcal{C}} p_{c,s}^{(t)} \cdot (h_{c,j,s}^{(t)})^2 + \sigma^2}, \quad (2.4)$$

where $p_j^{(t)}$ denotes the power per sub-carrier with which data is sent to terminal j , $p_{c,s}^{(t)}$ is the power with which cell c transmits on sub-carrier s , $h_{c,j,s}^{(t)}$ denotes terminal j 's channel gain versus cell c , and σ^2 denotes the noise power per sub-carrier.

2.5 Link-to-System Model

For the evaluation of the control channel reliability, i.e. to estimate the block error probability (BLEP) as a function of the link quality, we use the mutual information effective SINR metric (MIESM), which has been shown to achieve very high BLEP prediction accuracy in OFDM systems in [9]. That means that for each user, we calculate the SINR per allocated control channel sub-carrier according to (2.4) and compute the effective SINR value as follows:

$$\gamma_{\text{eff},j}^{(t)} = F_{\text{sinr2si}}^{-1} \left(\sum_{s \in \mathcal{S}} x_{c,j,s}^{(t)} \cdot F_{\text{sinr2si}}(\gamma_{j,s}^{(t)}) / (\phi_j \cdot l_L) \right), \quad (2.5)$$

where F_{sinr2si} (as shown in Figure 2.2) is a function that maps the user's received SINR to the related symbol-information value. Variable $x_{c,j,s}^{(t)}$ is the user/sub-carrier assignment that equals 1, if in cell c sub-carrier s is assigned to user j at t and 0 otherwise. The block error probability for this user is then determined by $F_{\text{sinr2blep}}(\gamma_{\text{eff},j}^{(t)}, \rho)$, where ρ is the per-user control channel code-rate. Note that if there is no set of values for a certain code-rate ρ , the set of the closest available code-rate is chosen. Inside the simulator, the error probability is translated into the error rate by means of random number drawing. In case of a control channel error, all related user data on the data channel is lost.

Chapter 3

Control Channel Configuration

We assume the control channel power per sub-carrier to be fixed - the maximum admitted transmission power p_{\max} is equally split and distributed among all sub-carriers: $p_{c,s} = p_{\max}/S$. Moreover, we assume the user terminal j to be able to measure the momentary SINR value per sub-carrier $\gamma_{j,s}^{(t)}$ and compute the average over all sub-carriers $\bar{\gamma}_j^{(t)}$. We require that this value is signaled to the connected base station, where it arrives being α TTIs old.

3.1 Static Coding Configuration

In case of the static coding configuration, the control channel size L , as well as the number of CCEs per user ϕ (and accordingly the per user code-rate ρ) are fixed in each simulation scenario. Note that only those users that have been selected for data delivery during the next TTI are assigned control channel resources. These users form the set of scheduled users in c , which we will refer to as $\mathcal{J}_c^{(t)}$, whereas the number of users in $\mathcal{J}_c^{(t)}$ is denoted as $J_c^{(t)}$. The users in $\mathcal{J}_c^{(t)}$ are ordered according to their priority, which has previously been determined by the scheduler. Starting with the highest priority user ($j = 1$), the control-channel user/sub-carrier assignments in the logical domain of cell c are selected as follows:

$$\forall c : \begin{cases} x_{c,1,1} = \dots = x_{c,1,\phi \cdot l_L} = 1, \\ x_{c,2,\phi \cdot l_L + 1} = \dots = x_{c,2,2 \cdot \phi \cdot l_L} = 1, \\ \vdots \\ x_{c,J_c,(J_c-1) \cdot \phi \cdot l_L + 1} = \dots = x_{c,2,J_c \cdot \phi \cdot l_L} = 1, \end{cases}$$

all other $x_{c,j,s} = 0$. Note that the number of available CCEs per TTI is limited. In case there are too few CCEs available in order to assign ϕ CCEs to all scheduled users ($N < J_c \cdot \phi \cdot l_L$), ϕ CCEs are assigned to as many users as possible, one user is assigned the remaining CCEs, and all other users, if any, do not get any control channel capacity in this TTI.

```

Initialize:  $isDone = false, p_j = p_{tot}/S \forall j \in \mathcal{J}$ 

1 for ( $L = 1; L \leq 3; L ++$ ) do
2    $\forall \{j, s\} \in \mathcal{J} \times \mathcal{S} : x_{c,j,s} = 0$ 
3    $s_{tot} = 0$ 
4   for ( $j = 1; j \leq J_c; j ++$ ) do
5     for ( $s = 1; s \leq (S - s_{tot}); s = s + l_L$ ) do
6        $x_{c,j,s+s_{tot}} = \dots = x_{c,j,s+s_{tot}+l_L-1} = 1$ 
7        $\varphi_j^{(t)} = \Psi_{DL}/2 \cdot L \cdot (s + l_L)$ 
8       if ( $F_{sir2bler}(\bar{\gamma}_j^{(t-\alpha)}, \varphi_j^{(t)}) \leq \hat{P}_B$ ) then
9         if ( $((s + l_L)/l_L) \in \{1, 2, 4, 8\}$ ) then
10           $s_{tot} = s_{tot} + s + l_L$ 
11          if ( $j == J_c$ ) then
12             $isDone = true$ 
13            end
14            break
15          end
16        end
17      end
18    end
19  end
20  if ( $isDone$ ) then
21     $break$ 
22  end
23 end

```

Algorithm 1: Control data dynamic coding algorithm.

3.2 Dynamic Coding Configuration

In the dynamic coding case, the control channel size L and the number of CCEs per user ϕ_j (and accordingly the per user code-rate ρ_j) are individually determined by each base-station per TTI. In order to enable the receiver to handle the varying control channel size, two bits per TTI are used to signal L . Blind detection at the receiver side allows for different combinations of coding-rates per user. However, since blind detection mechanisms require high computational power, we restrict our selection of the number of CCEs per user ϕ_j to be exclusively out of the set $\{1, 2, 4, 8\}$ (in accordance with [10]). Again, note that only those users that have been selected for data delivery during the next TTI are assigned control channel resources. In order to reach the dynamic coding goal - achieving control channel robustness with a minimum amount of redundancy - Algorithm 1 is executed once per TTI in each base-station c :

Initially, the smallest available control channel size $L = 1$ is selected. As a consequence, each CCE is composed of $l_L = \varphi$ sub-carriers. In Step 2 and 3, all user/sub-carrier assignments in cell c are reset and the overall number of assigned sub-carriers s_{tot} is set to zero. Then, inside the loop that comprises Steps 5–13, for each user as many CCEs as necessary to achieve an expected block error probability (BLER) smaller than the target BLER \hat{P}_B are assigned. Note that in each iteration the sub-carrier counter s is increased by the number of sub-carriers per CCE (Step 5). Thus, in each iteration a complete CCE is assigned in Step 6. In Step 7 the momentary code-rate of user j is calculated according to Equation (2.3). Using this momentary code-rate and the α TTIs old average SINR value over all sub-carriers $\bar{\gamma}_j^{(t-\alpha)}$, which has previously been provided by terminal j , the expected BLER is determined by $F_{\text{sir2bler}}(\bar{\gamma}_j^{(t-\alpha)}, \varphi_j^{(t)})$. It is compared to the target BLER \hat{P}_B in Step 8. If the expected BLER is larger than the target BLER value, another CCE is assigned by going over Steps 5 through 7 again. If it is smaller, it is checked in Step 9, whether a valid number of CCEs has been assigned to j . If this is not the case, more CCEs are assigned. Once a valid number of CCEs yields an expected BLER that is smaller than the target BLER, user j 's assignment is done. Then, in Step 10 the overall number of assigned sub-carriers s_{tot} is updated accordingly. If j is the user of least priority (i.e. the last user to be scheduled), the process is marked as finished using the *isDone* flag in Step 12, before the loop is broken in Step 13. Arriving at Step 14, two different states need to be distinguished: either all users fulfill the requirement that their expected BLER is smaller than the target BLER - in this case the assignment process is finished and the main loop broken (Step 15), or the momentary available number of CCEs is too small to meet all users' requirements. In the latter case, the complete process is repeated with an increased L . In the very rare case that even for $L = 3$ there is one or more users that do not get enough resources, those users are neglected.

Chapter 4

Simulation

We have performed our simulations on an LTE system-level simulator developed at Ericsson, which implements the system-, channel-, and link-to-system models described in Section 2. The system parameterization follows an urban indoor-user scenario with an inter site distance of $d = 500\text{m}$ and a down-link bandwidth of $B_{\text{DL}} = 10\text{ MHz}$. With exception of the number of cells that – due to simulation complexity reasons – we have set to 9, our scenario follows case 1 of [11]. All additional simulation parameters are listed in Table 4.1.

4.1 Methodology

We have chosen the base station schedulers to be priority weight based schedulers, where the priorities depend on the users' packet delay and channel state values. Note that the co-channel interference (CCI) impact on the control channel depends on the control channel load, which depends on the number of scheduled users per cell J_c . Thus, we have varied the CCI impact on the control channel by influencing the scheduler's resource allocation decisions: in each TTI a certain maximum data channel resource share per-user κ is applied. A choice of $\kappa = 1/3$ restricts the scheduler to provide a maximum of one third of all data-channel resources of this TTI to a single user. As a consequence at least three users are scheduled, if available in the cell. Note that we assume full buffers for all users in the system, such that there is a perpetual need for each user to be scheduled. We have simulated a high, a medium, and a low control channel load scenario (see Table 4.1). An example scenario for high control channel load consists of a system that is mainly utilized by VoIP users, whereas scheduling decisions in a system that is biased towards FTP users usually yields low control channel load. For the static coding case, we have additionally varied the number of CCEs per user ϕ and the control channel size L amongst the different simulation scenarios. An overall number of 50.000 TTIs (5 iterations with 10.000 TTIs each) have been simulated per scenario.

4.2 Results

The Figures 4.1 and 4.2 show the results of the dynamic coding approach, as well as the results of selected static coding scenarios. Low control channel load results with an average number of 0.9

Parameter	Symbol	Value
Overall number of cells	C	9
Overall number of users	J	45
Overall number of sub-carriers	S	600
Downlink assignment size in bits	Ψ_{DL}	40
Cntr. channel size in OFDM symb.	L	1,2,3
Cntr. channel elem. (CCE) per user	ϕ	1,2,4,8
CCE size in resource elem. (REs)	φ	36
Max. user resource share per TTI	κ	$\frac{1}{5}, \frac{1}{3}, 1$
Max. transmission power per cell	p_{max}	46 dBm
Target block error rate (BLER)	\hat{P}_B	0.01
Reporting delay	α	1

Table 4.1: Simulation Parameters.

scheduled users per cell and TTI are shown on the top, high load results with an average of 4.5 scheduled users per cell and TTI are shown at the bottom of the respective Figure. We have selected those static coding scenarios for presentation that show the best BLER performance in the respective load case. In addition, we have included some curves that help us pointing up various aspects in the present results.

From the result graphs of the low load scenario it can be stated, that 90% of all users already have a block error rate (BLER) that corresponds to the chosen per-user system target error probability $\hat{P}_B = 0.01$, if statically one CCE per user is assigned ($\phi = 1$, corresponding to a per-user code-rate of approximately $\rho = 1/2$). The results for different control channel sizes L are similar for $\phi = 1$. As expected, the BLER decreases with an increasing number of CCEs (i.e. stronger coding) in the case $L = 2$ (transition from $\phi = 1$ to $\phi = 2$). However, note that for $L = 1$ the BLER gets worse when the redundancy is increased from $\phi = 2$ to $\phi = 4$ CCEs per user. This is mainly due to the fact that the impact of co-channel interference (CCI) grows with the fraction of used sub-carriers, which is proportional to ϕ , but anti-proportional to L . In the latter case, the coding gain does not balance the increased CCI. This trend is even more visible in the graphs of the high load case. Here, the coding gain when switching from $\phi = 1$ to $\phi = 2$ in the $L = 2$ case – which accounts for better BLER performance at low load – leads to worse performance, whereas switching from $\phi = 2$ to $\phi = 8$ if $L = 3$ leads to the only scenario, where 90% of the users have a BLER performance that is at least in the order of magnitude of the target BLER \hat{P}_B . Thus, it must be reasoned that in the static coding case the control channel size L , as well as the number of CCEs per user ϕ must be carefully chosen with respect to the expected control channel load (that mainly depends on the scheduling strategy). Stronger code-rates might lead to a worse BLER performance.

Accordingly good are the results of the dynamic coding approach. From the low load BLER graph it can be seen that its BLER performance approximately corresponds to the performance of the strongest static coding case ($L = 3, \phi = 8$): more than 90% of all users do not experience any block error at all. In the high load case (bottom), the dynamic coding approach significantly outperforms

the strongest coding case. This is mainly due to the fact that the CCI generating impact of additional redundancy is minimized, if the coding rate is adapted on a per user basis. In other words, the probability of two sub-carriers being used in neighboring cells is much lower than in the strongest static case, whereas the probability of having enough redundancy in order to decode the signaling information at the receiver is much higher than in the weakest coding case. Consequently, the adaptive coding approach has a much better BLER performance, which is translated into an average per user throughput that is close to the ideal case, as can be seen in Figure 4.2's lower graph. Here, a system that relies on an ideal (error-free and zero-resource consuming) control channel is referred to as *ideal*. The superiority of the adaptive coding approach is not that obviously visible in the low load scenario's average throughput graph (on top). Here, weak static coding approaches (e.g. $L = 1, \phi = 1$) deliver throughput results that are as good. Explicit gains are present for the best 10% of the users only (some other might even experience slightly worse performance). This is mainly due to the fact that in the low load scenario all shown combinations perform well in terms of BLER performance. Thus, the differences in average per user throughput between the different static approaches is solely the difference in redundancy that affect the data channel capacity. Compared to the weak static coding cases, the amount of redundancy used in the adaptive coding approach is never smaller, and, thus, there is no chance for adaptive coding to perform significantly better in terms of per user data throughput. Still, adaptive coding performs as good, and, thus, the advantage of not having to decide on a single coding rate that most probably has to cope with different load scenarios is valid.

In Figure 4.3 we compare the dynamic coding approach performance with the performance of a similarly configured system using static coding but dynamic power allocation at the transmitter. To do so, we utilize a dynamic power loading algorithm that has been introduced in [7]. For the dynamic power case, the coding configuration ($L = 1, \phi = 2$) that delivers the best BLER performance in the medium and high load scenarios was chosen. From the graphs it can be seen that even though the adaptive coding approach delivers slightly better BLER results, both approaches perform the same in terms of average per user data throughput. As a consequence, at this point there is no reason to prefer one of the two when it comes to implementing an according system. However, as mentioned before, the adaptive coding algorithm depends on blind detection at the receiver side, whereas the adopted dynamic power algorithm relies on information storage and processing at the transmitter side. Moreover, the two algorithms consist of algorithmic steps of significantly differing computational complexity. In order to decide on which approach to prefer for a real-world application, an exhaustive complexity analysis needs to be conducted. This kind of analysis, however, lies beyond the scope of this paper.

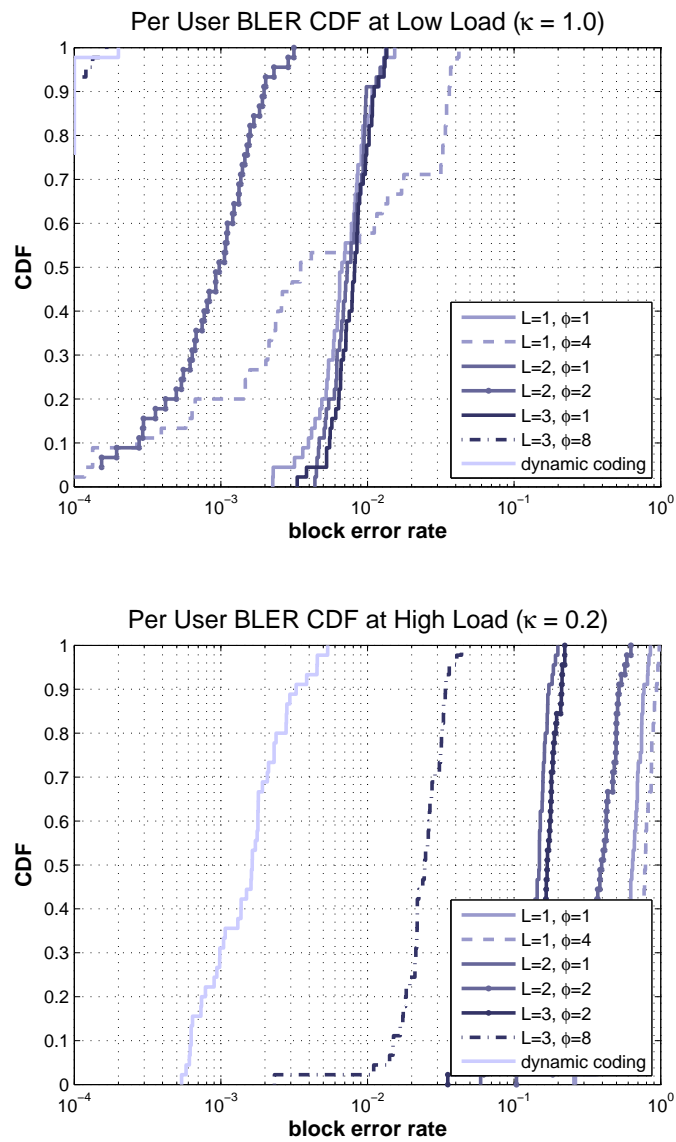


Figure 4.1: The simulation result graphs show the cumulative distribution functions (CDFs) of the per user block error rate for the dynamic coding and selected static coding scenarios. Two different load cases are illustrated: low control channel load ($\kappa = 1.0$, in average 0.9 scheduled users per cell and TTI – top) and high control channel load ($\kappa = 0.2$, in average 4.5 scheduled users per cell and TTI – bottom).

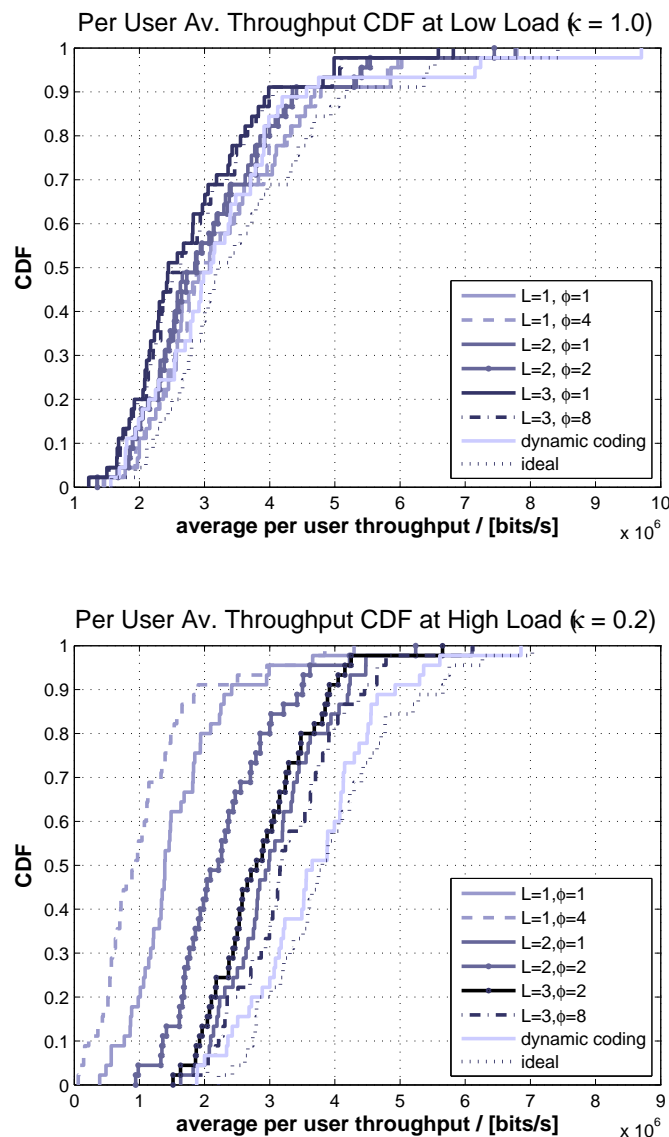


Figure 4.2: The simulation result graphs show the cumulative distribution functions (CDFs) of the per user throughput for the dynamic coding and selected static coding scenarios. Two different load cases are illustrated: low control channel load ($\kappa = 1.0$, in average 0.9 scheduled users per cell and TTI – top) and high control channel load ($\kappa = 0.2$, in average 4.5 scheduled users per cell and TTI – bottom). The curves that are labeled 'ideal' show the throughput values for according systems that rely on an ideal (error-free and zero-resource consuming) control channel.

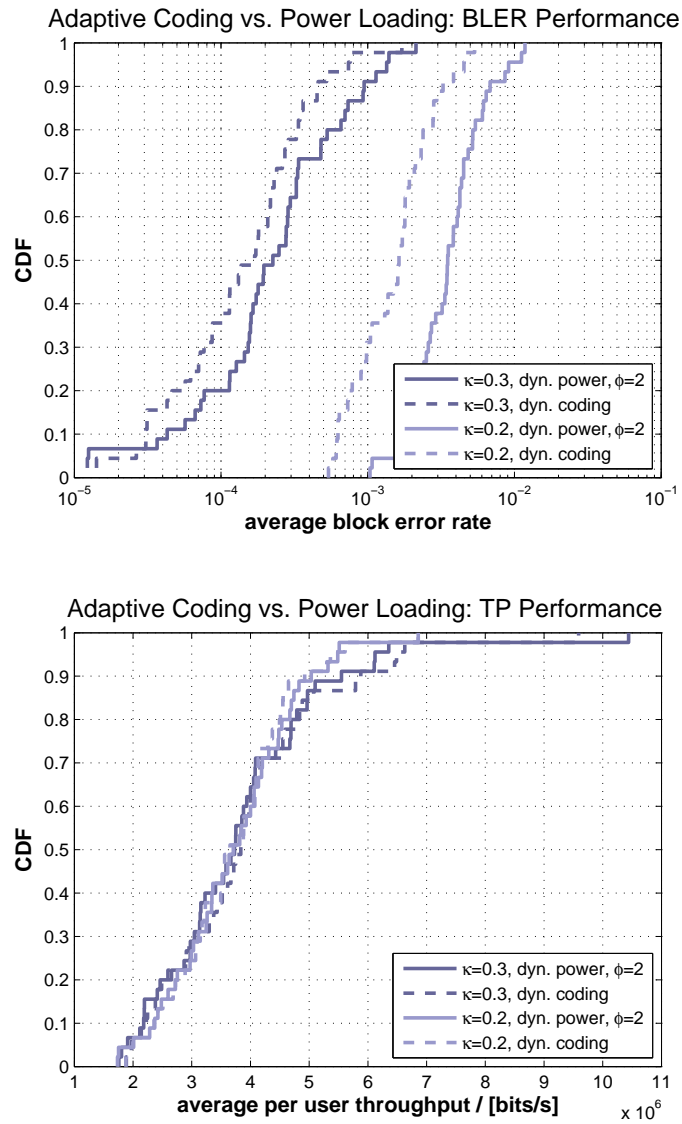


Figure 4.3: The difference in block error rate (top) and user data throughput (bottom) between the dynamic coding approach and the best performing combination of control channel size and number of CCE per user ($L = 1, \phi = 2$) of the dynamic power approach as introduced in [7]. The graphs show the results for the medium ($\kappa = 1/3$), and the high ($\kappa = 1/5$) load scenario.

Chapter 5

Conclusions

We have investigated the performance of a dynamic multi-user OFDM system that depends on an unreliable control channel. Two different scenarios have been compared: the straight forward static coding approach, and an adaptive coding approach. In both cases, a limited set of available code-rates has been examined, where the chosen code rate was static per scenario and the same for all users in the first, but flexible in the latter case. We have shown that the application of the newly introduced adaptive coding algorithm delivers significant block error rate performance gains in all investigated cases. This gain translates into significant per user data throughput gains compared to all possible static code-rate combinations in a high control channel load scenario. The gains are smaller in low load situations. In addition, if adaptive coding is used, there is the advantage of not having to decide on a single coding configuration, which most probable has to cope with different load scenarios.

Moreover, we have compared our dynamic coding approach to an existing dynamic power allocation approach that has previously been introduced with the same target (reliable control channel data delivery for each user, while minimizing the control channel resource requirement). We have shown that dynamic coding yields superior BLER performance. However, since the BLER performance of both approaches lies in reasonable bounds, this superiority cannot be translated into throughput gains, i.e. the two are equivalent in terms of per data throughput. Consequently, the approach causing lower additional cost should be considered for implementation in an according real-life system. However, so far little is known about computational complexity of the two. For this reason, we suggest an exhaustive complexity analysis of both approaches as future work issue.

Bibliography

- [1] C.Y. Wong, R.S. Cheng, K.B. Letaief, and R. Murch, "Multiuser OFDM with adaptive subcarrier, bit and power allocation," *IEEE Journal on Selected Areas of Comm.*, vol. 17, no. 10, pp. 1747–1758, Oct 1999.
- [2] W. Rhee and J. Cioffi, "Increase in capacity of multiuser OFDM system using dynamic sub-channel allocation," in *Proc. Vehicular Technology Conference (VTC)*, 2000, pp. 1085 – 1089.
- [3] S. Pietrzyk and G.J.M Janssen, "Subcarrier allocation and power control for qos provision in the presence of cci for the downlink of cellular ofdma systems," in *Proc. of the IEEE Vehicular Technology Conference (VTC, Spring 2003)*, Jeju, Korea, Apr. 2003, vol. 4.
- [4] M. Bohge, J. Gross, and A. Wolisz, "The potential of dynamic power and sub-carrier assignments in multi-user OFDM-FDMA cells," in *Proc. of IEEE Global Communications Conference (Globecom) 2005*, St. Louis, MO, USA, Nov. 2005.
- [5] J. Gross, H. Geerdes, H. Karl, and A. Wolisz, "Performance analysis of dynamic OFDMA systems with inband signaling," *IEEE JSAC, Special Issue on 4G Wireless Systems*, Mar. 2006.
- [6] J. Gross, P. Alvarez, and A. Wolisz, "The signaling overhead in dynamic OFDMA systems: Reduction by exploiting frequency correlation," in *Proc. of the IEEE International Conference on Communications (ICC 2007)*, Glasgow, Scotland, June 2007.
- [7] M. Bohge, A. Wolisz, A. Furuskr, and M. Lundevall, "Multi-user OFDM system performance subject to control channel reliability in a multi-cell environment," submitted to the IEEE 2008 International Communications Conference (ICC '08), Beijing, China.
- [8] 3GPP: TS 36.211, "Technical specification group radio access network; physical channels and modulation (release 8)," June 2007, Version 1.2.0.
- [9] K. Brueninghaus, D. Astely, T. Salzer, S. Visuri, A. Alexiou, S. Karger, and G.-A. Seraji, "Link performance models for system level simulations of broadband radio access systems," in *Proc. of the 16th IEEE International Symposium on Personal, Indoor, and Mobile Radio Communications (PIMRC 2005)*, Berlin, Germany, Sept. 2005, vol. 4.
- [10] 3GPP: R1-071820, "DL control channel structure," Apr. 2007.
- [11] 3GPP: TR 25.814, "Physical layer aspects for evolved UTRA (release 7)," Sept. 2006, Version 7.1.0.